

PREPARATION OF MAGNETIC-ZnO NANOCOMPOSITE BY HIGH ENERGY MILLING METHOD FOR METHYL ORANGE DEGRADATION

(PEMBUATAN NANOKOMPOSIT MAGNET-ZnO DENGAN METODA HIGH ENERGY MILLING UNTUK DEGRADASI METHYL ORANGE)

Didin S. Winatapura, Siti Wardiyati, and Adel Fisli

Pusat Sains dan Teknologi Bahan Maju – Badan Tenaga Nuklir Nasional
Gd. 42 Kawasan Puspiptek, Serpong, Tangerang 15314 – Indonesia.

E-mail: didinsw@batan.go.id

Received: 8 Juli 2016; revised: 18 September 2016; accepted: 29 September 2016

ABSTRACT

A magnetic Fe₃O₄/ZnO nanocomposite (NCs) was prepared by a high energy milling (HEM) method. In the present study, the ZnO catalyst was prepared through two ways. The ZnO was synthesized by coprecipitation method (ZnO (S)), and ZnO directly used a commercial product (ZnO (Ald)). The prepared NCs were characterized using X-ray diffraction (XRD), vibrating sample magnetometer (VSM), Fourier transform infrared (FTIR), transmission electron microscope (TEM), and UV-Vis spectrophotometer. The XRD refinement indicates that Fe₃O₄ nanoparticle (NP) is a single phase and well indexed to cubic spinel structured magnetite. The Fe₃O₄/ZnO (S) and Fe₃O₄/ZnO (Ald) NCs are consisted of Fe₃O₄ and ZnO phases. The VSM result show that Fe₃O₄ NP, Fe₃O₄/ZnO (S), and Fe₃O₄/ZnO (Ald) NCs possess super-paramagnetic properties with saturation magnetization (M_s) is 102 emu.g⁻¹, 28 emu.g⁻¹ and 26 emu.g⁻¹, respectively. The TEM observation shows that the average diameter of Fe₃O₄ is approximately 15 nm, while the thickness both of ZnO shell is ranging 20 nm - 50 nm. The average diameter of TiO₂ P25 particle as catalyst was observed about 20 nm. The photocatalytic activity of catalysts were evaluated based on the degradation of methyl orange (MO) dye solution. The result shows that at pH = 7, the Fe₃O₄/ZnO (Ald) NC can degrade the pollutant in MO dye solution to 99 %, where as at pH = 3, the catalyst TiO₂ P25 degrade only 96%.

Keywords: Fe₃O₄/ZnO nanocomposite, High energy milling, Degradation, Methyl orange, Photo-catalytic

ABSTRAK

Nanokomposit magnet Fe₃O₄/ZnO (NK) dibuat menggunakan metoda *High Energy Milling (HEM)*. Pada penelitian kali ini, katalis ZnO disiapkan melalui dua metode. ZnO dibuat dengan metode kopresipitasi ZnO (S), dan katalis ZnO dipakai langsung dari produk komersial (ZnO (Ald)). NK yang dihasilkan dikarakterisasi menggunakan *X-ray diffraction (XRD)*, *vibrating sample magnetometer (VSM)*, *Fourier transform infrared (FTIR)*, *transmission electron microscope (TEM)* dan *UV-Vis spectrophotometer*. Hasil *refinement XRD* memperlihatkan bahwa Fe₃O₄ berfase tunggal dan terindeks baik untuk magnet berstruktur *spinel* kubik. NK Fe₃O₄/ZnO (S) dan Fe₃O₄/ZnO (Ald) tersusun dari fase Fe₃O₄ dan ZnO. Hasil pengukuran sampel dengan *VSM* menunjukkan bahwa Fe₃O₄, Fe₃O₄/ZnO (S) dan Fe₃O₄/ZnO (Ald) berkelakuan *superparamagnetic* dengan menghasilkan magnet saturasi (M_s) masing-masing sebesar 102 emu.g⁻¹, 28 emu.g⁻¹ dan 26 emu.g⁻¹. Hasil pengamatan sampel dengan *TEM* menunjukkan bahwa diameter rata-rata Fe₃O₄ sekitar 15 nm, sedangkan ketebalan lapisan ZnO keduanya berkisar 20 nm - 50 nm. Ukuran diameter rata-rata partikel TiO₂ P25 teramati sekitar 20 nm. Aktivitas fotokatalik dievaluasi dengan mendegradasi larutan *methyl orange (MO)*. Hasil pengujian menunjukkan bahwa pada pH = 7, Fe₃O₄/ZnO (Ald) mampu mendegradasi larutan zat warna *MO* hingga 99 %, sedangkan pada pH= 3, katalis TiO₂ P25 hanya mampu mendegradasi 96 %.

Kata kunci: Nanokomposit Fe₃O₄/ZnO, *High energy milling*, Degradasi, *Methyl orange*, Fotokatalitik

INTRODUCTION

Metal oxide semiconductor photo-catalysts have been extensively studied in the fields of environmental purification. Among the various oxide semiconductor photo-catalysts

zinc oxide (ZnO), and titanium dioxide (TiO₂) from the commercial Degussa product P25 are widely used as materials for photo-catalytic processes, because of its high photosensitivity,

and environmentally friendly nature. ZnO and TiO₂ P25 have proven to be the most suitable materials for removing pollutants from the water with their high surface-to-volume ratio, high photosensitivity, good quantum efficiency, and non-toxic to the nature (Abdollahi et al. 2012; Álvarez et al. 2010). However, a main problem in industrial application of ZnO and TiO₂ P25 nanoparticles in slurry reactor system is the difficulties encountered in recollection of the nanoparticles from the treated waters. The separation step such as filtration is not enough to prevent the possible large scale loss and the potential secondary pollution caused by the loss ZnO and TiO₂ P25 nanoparticles (Abdollahi et al. 2012; Ahadpour Shal and Jafari 2014; Xu and Li 2014).

Recently, magnetically separable photo-catalysts of the Fe₃O₄/ZnO NCs have attracted attention because of their scientific and technological importance in the environmental purification (Feng et al. 2014; Nikazar et al. 2014). In this case, both the Fe₃O₄ magnetic core and the ZnO shell are of interest. The incorporation of Fe₃O₄ magnetic core into the semiconductor ZnO possesses the property not only of high surface area to volume ratio but also the magnetic photo-catalysts have dual functions. Fe₃O₄ magnetic component can be easily and effectively collected the catalysts with the help of a magnetic field, and the photo-catalytic properties of ZnO shell can eliminate the organic pollutants in the wastewater.

Several methods have been already established for the preparation of magnetic photo-catalyst and their photo-catalytic properties. Nikazar et al. (2014) used precipitation method for preparation of Fe₃O₄/ZnO NCs, and Feng et al. (2014), fabricated the Fe₃O₄/ZnO by dehydrating zinc acetate in the present of Fe₃O₄ NPs in diethylene glycol. Both of Fe₃O₄/ZnO NPs exhibited a high activity photo-catalytic for phenol degradation.

Recently, Winatapura et al., (2016) have performed the Fe₃O₄/ZnO using Zn(CH₃COO)₂·2H₂O precursor to make ZnO nanoparticles for methylene blue degradation.

In this work is focused that the magnetic Fe₃O₄/ZnO NCs were produced by a mechanochemical activation using high energy milling (HEM) process for methyl orange (MO) degradation. It is well known that the mechanochemical or the activation of chemical reactions by mechanical energy can lead many applications, it is from waste processing to the production of advanced materials and enhanced mechanical properties (Giwa et al. 2012; Iwasaki et al. 2010).

The ZnO NP as a catalyst is obtained in two ways. Firstly, ZnO is made from ZnCl₂·6H₂O precursor using coprecipitation method. Secondly, the ZnO was taken from a commercial product (Sigma-Aldrich) without further purification. The weight percent ratio between ZnO and Fe₃O₄ is arranged of 1 : 4. The obtained Fe₃O₄/ZnO NCs were annealed at 550°C for 2 hours, and then characterized using X-rays diffractometer, vibrating sample magnetometer, transmission electron microscope, and UV-Vis spectrophotometer. The photo-catalytic efficiency of Fe₃O₄/ZnO NCs at different pH solution of MO dye photodegradation was reported. These results were compared with the TiO₂ catalyst from commercial Degussa product P25 (Germany). In the frame of this research TiO₂ P25 was used as comparative material.

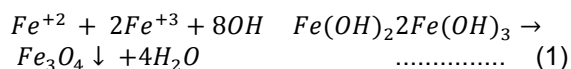
MATERIALS AND METHOD

Materials

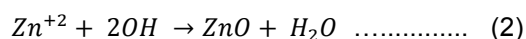
FeCl₃·6H₂O, FeCl₂·4H₂O, HCl, Methyl orange (MO), NaOH, NH₄OH and ZnCl₂·6H₂O are Merck products. Commercial ZnO (≥ 99.0 %) powder is Sigma Aldrich and TiO₂ from commercial Degussa product P25 (Germany).

Methods

The Fe₃O₄ NPs were synthesized with coprecipitation method using iron (III) chloride, FeCl₃·6H₂O and iron (II) chloride, FeCl₂·4H₂O with molar ratio of 2 : 1 according to the method used by Winatapura et al. (2014) with modification. The synthesis was performed at 70°C using the 1-M NaOH and NH₄OH (25%) solution as precipitate agents. The chemical reaction of this process is written as follows (Ahadpour Shal and Jafari 2014):



The ZnO NPs was synthesis using coprecipitation method from ZnCl₂·6H₂O raw materials. In this work, 1-M of NaOH solution was added drop wise to ZnCl₂·6H₂O at 80 °C until pH= 12. The reaction can be written as:



The white precipitate was collected, purified with water and dried at 100 °C.

The preparation of Fe₃O₄/ZnO NCs was conducted by HEM (Certi-Prep 8000 M machine). The Fe₃O₄ NPs and ZnO powders (with 1 : 4 weights ratio) were mixed in a

Tungsten Carbide vial and milling for 10h. The weight ratio of Fe₃O₄/ZnO NCs and agate balls was arranged of 1 : 5. The Fe₃O₄/ZnO (S) NCs was annealed at 550 °C for 2h. This sample was labeled by Fe₃O₄/ZnO (S). The same procedure was then repeated for preparation of Fe₃O₄ and ZnO commercial product (Sigma Aldrich), and labeled with Fe₃O₄/ZnO (Ald). X-ray diffraction (XRD) patterns of the NCs were collected on a Pan-Analytical diffractometer with CuK α radiation ($\lambda = 0.154$ nm). The XRD data was analyzed using general structure analysis system (GSAS) (Larson and Von Dreele 2004). The magnetization of the sample was measured using a VSM (Oxford 1,2T). TEM images of NCs were obtained with a transmission electron microscope (JEOL JEM-1400) at an accelerating voltage of 120kV.

Photo-catalytic degradation of MO was performed in a slurry batch reactor which consisted of cylindrical beaker glass, magnetic stirrer and an UV-pen Ray 100 watt, $\lambda = 356$ nm (Model: UVP Pen Ray 90-0016-01), located at the center of the reactor. The distance between an UV-pen lamp and MO dye solution was arranged of about 5 cm. In all experiments, 100 mL MO dye in water solution of 30 ppm concentration was adjusted to pH 3 and pH 7. Then 0.1 g of each Fe₃O₄/ZnO (S) and Fe₃O₄/ZnO (Ald) NCs catalyst is added, and the mixture was stirred magnetically to obtain homogeneous suspension. Before irradiation, the reaction mixture was put in darkness for 3 h to achieve maximum adsorption of the MO onto the catalyst surface. After 3 h, a sample was taken and photocatalyst particles were separated using a magnetic bar. The 455 nm of MO dye concentration remaining was determined by UV-Vis spectrophotometer (Perkin-Elmer, Lambda 25) at a wavelength. These results are compared with TiO₂ P25 from the commercial Degussa product (Sigma Aldrich).

RESULTS AND DISCUSSION

The refinement result of XRD pattern of the prepared Fe₃O₄ NP, synthesized zinc oxide, ZnO (S) and zinc oxide commercial product (Sigma Aldrich), ZnO (Ald) are shown in Figure 1. In the XRD pattern of the prepared Fe₃O₄ NP, all diffraction peaks are well indexed to cubic spinel structured magnetite and appear at Bragg angles $2\theta \sim 30.23^\circ, 35.52^\circ, 43.03^\circ, 53.14^\circ, 57.02^\circ, 62.54^\circ$ corresponding to Miller indices (220), (311), (400), (422), (511), (440), according to JCPDS file no. 19-0629. Based on the Figure 1(a), the prepared growth orientation

of Fe₃O₄ lies along (311) crystallographic direction. It can be seen that the prepared Fe₃O₄ exhibit a single phase and no other peak associated with the impurity phase.

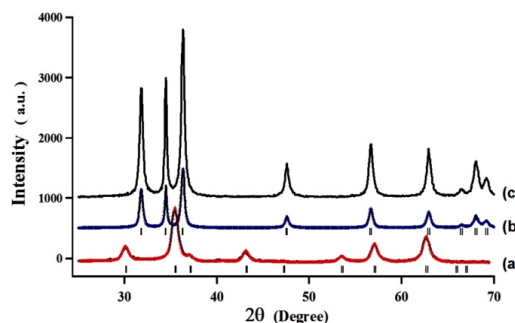


Figure 1. Refinement result of XRD pattern: (a) Fe₃O₄, (b) ZnO (S), and (c) ZnO (Ald) NPs

Fig. 1(b) and 1(c) show a refinement result of typical XRD pattern of prepared and the commercial zinc oxide, ZnO (S), and ZnO (Ald) NPs, respectively. Based on the Figure 1(b) and 1(c), the strong sharp peaks indicate that the ZnO (S) and ZnO (Ald) NPs are highly crystalline. The diffraction peaks of both ZnO are match with the standard data for a wurtzite structure (JPCDS 36-1451), and seemed at Bragg angles $2\theta \sim 31.85^\circ, 34.45^\circ, 36.35^\circ, 47.60^\circ, 56.70^\circ, 62.90^\circ, 66.55^\circ, 68.05^\circ, 69.20^\circ$ related to Miller indices (100), (002), (101), (102), (110), (103), (200), (112), (201). It is apparent from Figure 1(b) and 1(c) that both ZnO preparation results and the commercial product showed a single phase. A preferred growth orientation lies along the (101) crystallographic direction at $2\theta \sim 36.35^\circ$.

Figure 2 shows the refinement result of XRD Fe₃O₄/ZnO (S) and Fe₃O₄/ZnO (Ald) NCs produced very good quality of fitting with R factor is very small, and goodness of fit value χ^2 (*chi-squared*). It is seem that all the diffraction peaks can be readily indexed to Fe₃O₄ and ZnO phases. The diffraction peaks of Fe₃O₄ phase are indexed by “-”, while peaks intensity of the ZnO phase that marked by “+”. Some peaks of intensity enhancement are detected due to peak overlapping, as seen in Fig. 2. This is in a good agreement with work done by Feng et al. (2014).

Fig. 3 presents magnetization M curve of prepared Fe₃O₄ NPs, before and after ZnO coating, versus applied field H between -10 and +10kOe measured by VSM. The magnetization saturation (M_s) value of Fe₃O₄ NPs measured at room temperature exhibits an excellent magnetic saturation (M_s) is around 102emu.g^{-1} (Fig. 3(a)). The magnetic property Fe₃O₄ NPs is super-paramagnetic behaviour with no coercivity due to their small size. The M_s Value was observed around 93 and 65emu.g^{-1} for Fe₃O₄ bulk and NPs, respectively (Wei et al. 2012). However,

the M_s Value of Fe_3O_4 NP then reduces to 28.00emu.g^{-1} and 25.75emu.g^{-1} for Fe_3O_4/ZnO (Ald) and Fe_3O_4/ZnO (S), respectively. The molar ratio between Fe_3O_4 and ZnO was arranged of 1: 4. It can be seen that the coating of ZnO did not change the super-paramagnetic properties of Fe_3O_4 NP. The reduction of the saturation magnetization results from the existence of nonmagnetic ZnO shell on the surface of Fe_3O_4 core NPs. The measurement result is displays in Table 1.

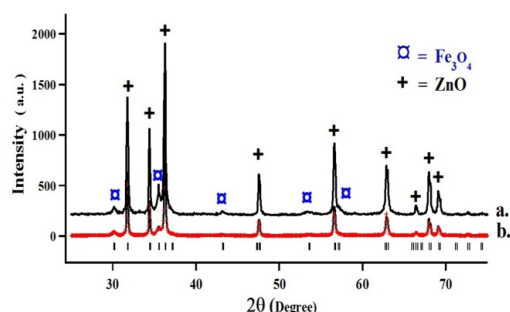


Figure 2. Refinement result of XRD pattern: (a) Fe_3O_4/ZnO (S), and (b) Fe_3O_4/ZnO (Ald) NCs

The TEM micrograph of prepared Fe_3O_4 NPs, Fe_3O_4/ZnO (S) NCs, Fe_3O_4/ZnO (Ald) NCs, and TiO_2 P25 Nps are presented in Fig. 4. The most of aggregated Fe_3O_4 particles are spherical; with the average size of the most particles is nearly 15nm, as seen in Fig. 4a. Fig. 4b and 4c show TEM image of Fe_3O_4/ZnO (S) and Fe_3O_4/ZnO (Ald) NCs. It can be seen clearly that the whole Fe_3O_4 NPs coated by the ZnO shell. The morphology of these Fe_3O_4/ZnO NCs was generally the same which shows a core-shell like structures. The dark part (black colour) of the Fe_3O_4/ZnO NCs is the Fe_3O_4 core and the ZnO shell is the light parts (grey colour), as it is seen in Fig. 4(b) and 4(c). The thickness of the ZnO shell in both of Fe_3O_4/ZnO (Ald) and Fe_3O_4/ZnO (S) is between 20-50nm. This result is in a good agreement with Choi et al. (2011), which the magnetic composite consist of nanoscale grains and has a super-paramagnetic

behaviour. TEM image of TiO_2 nanoparticles from commercial Degussa product P25 are shown in Fig. 4 (d). It is clear spherical and non homogenous structure can be seen in Fig. 4 (d) having diameter $\sim 20\text{nm}$.

The photo-catalytic activity was expressed by means of the degradation efficiencies of methyl orange (MO) dye for different catalysts and condition (pH = 3 and 7) are presented in Fig. 5 and 6.

This is due to the pH value of dye solution is an important parameter in photo-catalytic degradation reactions that are taking place on the surfaces of semiconductors. It determines the surface charge properties of the photo-catalyst and the adsorption behaviour of pollutants.

Based on Fig 5 (a) – (d), the degradation rate of MO dye solution is obtained about 96%, 80%, 70% and 2%, respectively, for TiO_2 P25, Fe_3O_4/ZnO (Ald), Fe_3O_4/ZnO (S), and noncatalyst after 180 minutes UV-irradiation. The results were described in Table 1. Non-catalyst experiment was performed in the absence of any photo-catalysts, showed the absence of photo-degradation of MO under these reaction conditions. It can be seen that photo-catalytic efficiency of the TiO_2 P25 NPs is more suitable in acidic condition than Fe_3O_4/ZnO (Ald), Fe_3O_4/ZnO (S) NCs catalysts.

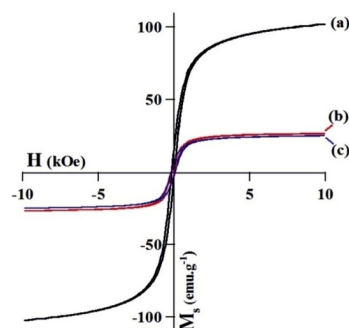


Figure 3. Magnetization curve of (a) Fe_3O_4 NPs, (b) Fe_3O_4/ZnO (Ald) and (c) Fe_3O_4/ZnO (S) NCs

Table 1. Parameters of degradation rate, apparent rate constant (k_{app}), and half life ($t_{1/2}$).

Catalyst	M_s (emu.g^{-1})	Deg. rate (%)		k_{app} (h^{-1})		$t_{1/2}$ (h)	
		pH=3	pH=7	pH=3	pH=7	pH=3	pH=7
Blank	-	2	3	-	-	-	-
TiO_2 P25	-	96	88	0.8732	0.7675	0.7938	0.6700
Fe_3O_4/ZnO (S)	26.00	70	96	0.3675	1.0337	1.8861	0.6705
Fe_3O_4/ZnO (Ald)	28.00	80	99	0.4557	1.3040	1.5211	0.5315
Fe_3O_4	102.00	-	-	-	-	-	-

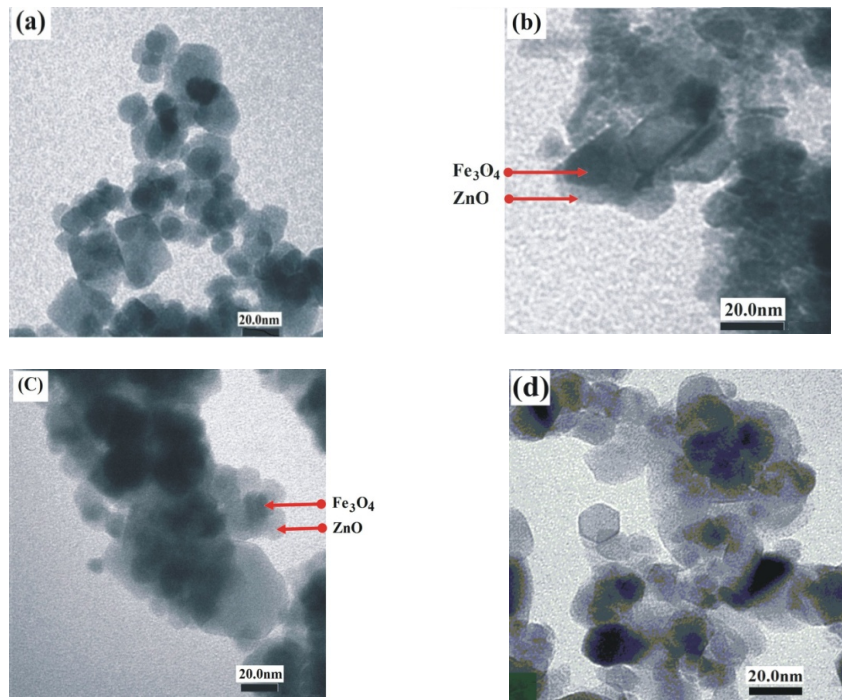


Figure 4. TEM micrograph of (a) Fe₃O₄ NPs, (b) Fe₃O₄/ZnO (S), and (c) Fe₃O₄/ZnO (Ald) NCs, and (d) TiO₂ P25 NPs.

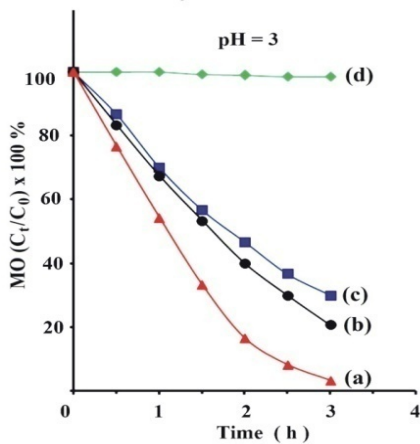


Figure 5. Degradation rate of MO dye solution in the dark and in the presence of different photo-catalyst under exposure to UV light at pH = 3 using (a). TiO₂ - P25, (b). Fe₃O₄/ZnO (Ald), (c). Fe₃O₄/ZnO (S) and (d). blank.

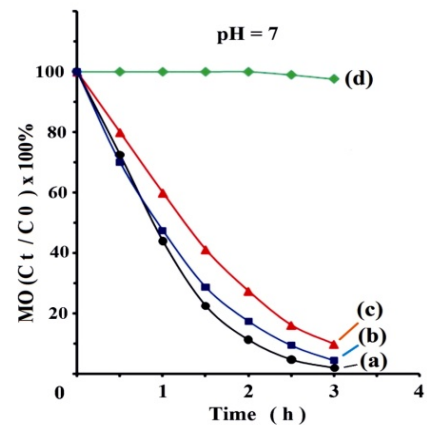


Figure 6. Degradation rate of MO dye solution in the dark and in the presence of different photo-catalyst under exposure to UV light at pH = 7 using (a). Fe₃O₄/ZnO (Ald), (b). Fe₃O₄/ZnO (S), (c). TiO₂-P25 and (d). blank.

It has been reported by Álvarez et al. (2010), Apopei et al. (2014), and Xue et al. (2013) that TiO₂ P25 has an excellent photo-activity for removal pollutants in pharmaceutical and personal care products, 4-Chlorophenol and pollutants in methyl orange from an aqueous solution. The high photo-catalytic activity of TiO₂ P25 is probably due to finer crystallite size (20-25nm), and BET specific surface area ~ 50m².g⁻¹ (Salazar 2010). Further, TiO₂ P25 has unique crystal structure, which is composed of anatase

(80%) and rutile (20%). In spite of TiO₂ P25 remains the most widely used photo-catalyst in water treatment, the difficulty in the recovery of the catalyst because of its small size to search alternative materials. The decreased of photocatalytic activity of the Fe₃O₄/ZnO in acidic condition is most likely due to the photocorrosion of ZnO. It has been reported that the zinc hydroxide surface (Zn-OH) can become charged by reacting with H⁺ (acidic environment) or OH⁻ (basic environment) ions due to surface amphoteric reactions (Abdollahi et al. 2012), Feng et al. 2014).

In contrast, the photo-catalytic efficiency of commercial and synthesized ZnO in Fe₃O₄/ZnO NCs in acidic condition is less favourable. Based on the Table 1., the degradation of MO dye solution by Fe₃O₄/ZnO (Ald) and Fe₃O₄/ZnO (S) NCs is obtained about 80% and 70%, respectively. The low of photo-catalytic efficiency of the ZnO in both samples Fe₃O₄/ZnO (Ald) and Fe₃O₄/ZnO (S) NCs can be attributed to the poor chemical stability of Fe₃O₄/ZnO NC in acidic environment (Abdollahi et al. 2012; Wei et al. 2012). Figure 6. shows the relationship between irradiation time and degradation rate of MO dye solution at pH = 7 treated by Fe₃O₄/ZnO (S), Fe₃O₄/ZnO (Ald), TiO₂ P25, and non-catalysts under UV light. Based on the Table 1., the degradation rate of MO dye solution is obtained of 99% for Fe₃O₄/ZnO (Ald) NCs, 96% for Fe₃O₄/ZnO (S) NCs with 0.1g/100ml (1g/L) respectively, and 88 % of TiO₂ P25 NPs. While the decolouration rate of the MO dyes without any catalysts is about 3 %. It is clear that at neutral condition (pH = 7) the photo-catalytic activities of the Fe₃O₄/ZnO (Ald), and Fe₃O₄/ZnO (S) NCs show a better performance than that of TiO₂ P25 after 180 minutes UV-irradiation.

In fact, the weight fraction of ZnO catalyst in the Fe₃O₄/ZnO (Ald) and Fe₃O₄/ZnO (S) NCs with TiO₂ Degussa P25 NPs is the same. It is suggested that mechanical energy can induce growth of nanocrystals in ZnO powder and change their surface properties so that affect significantly the photocatalytic activities of Fe₃O₄/ZnO NCs for methyl orange dye degradation in neutral condition. Beside that, the presence of magnetic Fe₃O₄ NPs with high M_s Value (102emu.g⁻¹) as the core in the ZnO system shell provides additional surface active site for adsorption of organic pollutants in MO dyes solution. This is consistent with the results conducted by Nikazar et al. (2014). They used precipitation method for Fe₃O₄/ZnO preparation, followed with calcinations temperature of 550 °C during 2h for phenol solution degradation after 5h UV-irradiation and produce high photo-catalytic activity.

The high photo-catalytic performance Fe₃O₄/ZnO NCs can be attributed to the different band gaps between ZnO (E_g = 3.37 eV) and Fe₃O₄ (E_g = 0.1 eV) and work function of ZnO and Fe₃O₄ which promote interfacial electron hole separation in the photo-catalytic process. The structural formula for magnetite is [Fe³⁺]_A [Fe³⁺,Fe²⁺]_B O₄, this particular arrangement of cations on the A and B sub-

lattice is called an inverse spinel structure (Ahadpour Shal and Jafari 2014). It has been reported that Fe³⁺ ions in Fe₃O₄ can act as photo-excited electron-trapping site to prevent the fast recombination photo-induced charge carriers, and also as a trigger for the enhanced photo-catalytic activity observed in Fe₃O₄-TiO₂ in visible light (Feng et al. 2014; Xu and Li 2014). Further, the Fe²⁺ ions which are relatively unstable in comparison with Fe³⁺ ions, react with the oxygen dissolved in the reaction mixture to generate Fe³⁺ ions and *O₂⁻ radicals. Thereby, it is obvious that the Fe₃O₄ magnetic core plays an important role in the photo-catalytic activity processes in the Fe₃O₄/ZnO NCs. Thus, the optimal photo-catalytic activity can be achieved only when the appropriate Fe content is added. Furthermore, due to the super-paramagnetic behaviour of Fe₃O₄, at least 0.085 g of the Fe₃O₄/ZnO NCs can be easily collected from the original 0.1 g of Fe₃O₄/ZnO.

The apparent first-order kinetic equation used to fit the experimental data was determined by equation (Wang, et al. 2012):

$$-\ln\left(\frac{C_t}{C_0}\right) = K_{app} \cdot t \quad \dots\dots (3)$$

Where K_{app} , is apparent rate constant, C_0 and C_t represent the initial concentration and concentration at particular time, t of MO dye solution. The half life ($t_{1/2}$) is determined by equation (A. Fisli 2014):

$$t_{1/2} = \ln 2 / K_{app} \quad \dots\dots\dots (4)$$

The corresponding linear transforms in $\ln(C_t/C_0)$ as a function of irradiation time are given in Fig. 7 and Fig. 8. At acidic environment (pH = 3), the TiO₂ P25 NPs decomposed the MO dye solution rapidly and completely in 180 minutes (Fig. 7). This phenomenon shows the highest photo-catalytic activity with the degradation rate constant (K_{app}) obtained of 0.8732 hour⁻¹ and the half life ($t_{1/2}$) is about 0.7938 hour, as seen in Table 1. It means that during $t_{1/2} = 0.7938$ hours (~ 47min.), the pollutants in MO dye solution decreased as much as 50% by TiO₂ P25 catalyst. In this condition Fe₃O₄/ZnO (S) dan Fe₃O₄/ZnO (Ald) NCs can degrade as much as 50% of pollutants in the dye MO in a longer time, during $t_{1/2} = 1.8861$ h⁻¹ (about 113 minutes) and $t_{1/2} = 1.5211$ h⁻¹ (about 91 minutes), respectively as presented in Table 1.

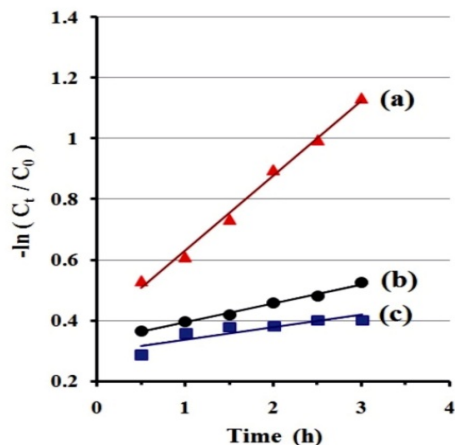


Figure 7. The kinetic curves of methyl orange dye disappearance for (a) TiO₂ P25 NPs, (b) Fe₃O₄/ZnO (Ald), and (c) Fe₃O₄/ZnO (S) NCs at pH = 3

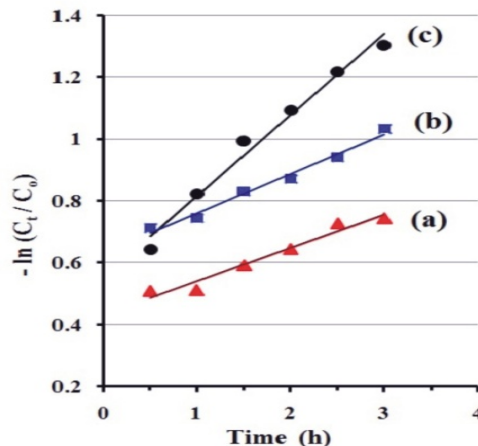


Figure 8. The kinetic curves of methyl orange dye disappearance for (a) TiO₂ P25 NPs, (b) Fe₃O₄/ZnO (S), and (c) Fe₃O₄/ZnO (Ald) NCs at pH = 7.

However, at pH = 7 the reaction rate of Fe₃O₄/ZnO (S) and Fe₃O₄/ZnO (Ald) NCs can degrade the MO dye solution completely up to 96% (Fig. 8b) and 99% (Fig. 8c), respectively in 180 minutes. The degradation rate constant (K_{app}) is achieved of 1.0337 hour⁻¹, and 1.1485 hour⁻¹ for Fe₃O₄/ZnO (S) and Fe₃O₄/ZnO (Ald) NCs, respectively. The half life ($t_{1/2}$) was obtained of $t_{1/2} = 0.6705$ (~ 47 minutes) and $t_{1/2} = 0.5315$ hours (~ 30 minutes) for Fe₃O₄/ZnO (S) and Fe₃O₄/ZnO (Ald) NCs, respectively. This means that, the Fe₃O₄/ZnO (Ald) NC can degrade the pollutants as much as 50% in MO dye solution is faster than the Fe₃O₄/ZnO (S) NC and TiO₂ P25 catalyst.

Based on the Figure 8a and 8b, we can obtain the same half life ($t_{1/2}$) for degradation process by TiO₂ P25 catalyst (Fig. 8a) and the Fe₃O₄/ZnO (S) NC (Fig. 8b). The values are $t_{1/2} = 0.6700$ hour and $t_{1/2} = 0.6705$ h (~ 47 min) for the degradation of the MO dye solution by TiO₂ P25 catalyst and the Fe₃O₄/ZnO (S) NC, respectively under UV light, see Table 1. The results show that their reaction rates are almost the same under UV-irradiation. Evidently, the degradation of MO dye solution decreases rapidly with increasing the reaction time which is indicated to the MO dye reduction from coloured aqueous to colourless.

CONCLUSION

It can be concluded high energy milling (HEM) process has been successfully prepared the Fe₃O₄/ZnO magnetic composites. The magnetic Fe₃O₄ was encapsulated with ZnO as-synthesized and the ZnO commercial (Sigma

Aldrich). XRD refinement result and TEM image interpreted that ZnO coated Fe₃O₄ are formed. TEM images indicate that the average particle size of aggregated Fe₃O₄ NP about 15nm, and the thickness of the ZnO shell in both of Fe₃O₄/ZnO (Ald) and Fe₃O₄/ZnO (S) NCs is between 20-50nm. The VSM measurement show that the Fe₃O₄ NP, Fe₃O₄/ZnO (Ald) and Fe₃O₄/ZnO (S) NCs possess super-paramagnetic behaviour, with magnetic saturation (M_s) value are 102emu.g⁻¹, 28emu.g⁻¹, and 26emu.g⁻¹, respectively.

Under acidic condition (pH ≤ 3), TiO₂ P25 can degrade the MO dye solution up to 96% higher when compared to Fe₃O₄/ZnO (Ald) and Fe₃O₄/ZnO (S) NCs. However, the photocatalytic activities of both Fe₃O₄/ZnO (S) and Fe₃O₄/ZnO (Ald) NCs appear to the most effective for removal of MO dye solution at neutral environment (pH = 7). In this condition, the mechanical energy can induce the growth of nanocrystals in zinc oxide powder, and change their surface properties. As a result, they can remove almost of the pollutants in the methyl orange (MO) dye solution. Furthermore, the Fe₃O₄/ZnO NCs can be easily collected and separated from the solution after the treatment process using a magnetic bar.

ACKNOWLEDGEMENT

This research was supported by "Research and Development of Smart magnetic and Magnetic Oxide Programme for DIPA Grants 2016" at Centre for Science and Technology of Advanced Materials – National Nuclear Energy Agency, Republic of Indonesia.

REFERENCES

- Abdollahi, Y., A.I H. Abdullah, Z. Zainal, and N. A. Yusof. 2012. Photocatalytic Degradation of P-Cresol by Zinc Oxide under UV Irradiation. *International Journal of Molecular Sciences* 13 (1): 302–15. doi:10.3390/ijms13010302.
- Ahadpour S., Alireza, and A. Jafari. 2014. Study of Structural and Magnetic Properties of Superparamagnetic Fe₃O₄-ZnO Core-Shell Nanoparticles. *Journal of Superconductivity and Novel Magnetism* 27 (6): 1531–38. doi:10.1007/s10948-013-2469-9.
- Álvarez, P. M., J. Jaramillo, F. López-Piñero, and P. K. Plucinski. 2010. Preparation and Characterization of Magnetic TiO₂ Nanoparticles and Their Utilization for the Degradation of Emerging Pollutants in Water. *Applied Catalysis B: Environmental* 100 (1–2): 338–45. doi:10.1016/j.apcatb.2010.08.010.
- Apopei, P., C. Catrinescu, C. Teodosiu, and S. Royer. 2014. Mixed-Phase TiO₂ Photocatalysts: Crystalline Phase Isolation and Reconstruction, Characterization and Photocatalytic Activity in the Oxidation of 4-Chlorophenol from Aqueous Effluents. *Applied Catalysis B: Environmental* 160–161 (1). Elsevier B.V.: 374–82. doi:10.1016/j.apcatb.2014.05.030.
- Choi, K.H, W.S Chae, E.M Kim, J.H Jun, and Y.R Kim. 2011. A Facile Fabrication of Fe₃O₄/ZnO Core-Shell Submicron Particles With Controlled Size. *IEEE TRANSACTIONS ON MAGNETICS, VOL. 47, NO. 10, OCTOBER* 47 (10): 1–4.
- Feng, X., H. Guo, K. Patel, H. Zhou, and Xia Lou. 2014. High Performance, Recovable Fe₃O₄-ZnO Nanoparticles for Enhanced Photocatalytic Degradation of Phenol. *Chemical Engineering Journal* 244: 327–34.
- Fisli. A. 2014. The Development of (Fe₃O₄/SiO₂/TiO₂) Magnetic Photocatalyst for Elimination of Organic Substances (Methylene Blue and Paraquat) in Water, Ph. D. Thesis, at The Graduate Program University of Indonesia, Indonesia. *Ph.D. Thesis*.
- Giwa, A., P. O. Nkeonye, K. A. Bello, and K. A. Kolawole. 2012. Photocatalytic Decolorization and Degradation of C. I. Basic Blue 41 Using TiO₂ Nanoparticles. *Journal of Environmental Protection*. 3: 1063–69.
- Iwasaki, T., K. Kosaka, S. Watano, T. Yanagida, and T. Kawai. 2010. Novel Environmentally Friendly Synthesis of Superparamagnetic Magnetite Nanoparticles Using Mechanochemical Effect. *Materials Research Bulletin* 45 (4):481–85. doi:10.1016/j.materresbull.2009.11.006
- Larson, A. C., and R.B. Von Dreele. 2004. General Structure Analysis System (GSAS), Los Alamos National Laboratory Report LAUR (2004), Pp. 86-748 .
- Nikazar, M., M. Alizadeh, R. Lalavi, and M. Rostami. 2014. The Optimum Conditions for Synthesis of Fe₃O₄/ZnO Core/shell Magnetic Nanoparticles for Photodegradation of Phenol. *Journal of Environmental Health Science and Engineering* 12 (1): 12–21. doi:10.1186/2052-336X-12-21.
- Salazar, M.J.G. 2010. Development and Application of Titanium Dioxide Coated Magnetic Particles for Photocatalytic Oxidation of Aqueous Phase Organic Pollutants.
- Wang, Z., L. Shen, and S. Zhu. 2012. Synthesis of Core-Shell Fe₃O₄-SiO₂-TiO₂ Microspheres and Their Application as Recyclable Photocatalysts. *International Journal of Photoenergy* 2012. doi:10.1155/2012/202519.
- Wei, Y., B. Han, X. Hu, Y. Lin, X. Wang, and X. Deng. 2012. Synthesis of Fe₃O₄Nanoparticles and Their Magnetic Properties. *Procedia Engineering* 27: 632–37.
- Winatapura, D.S, S.H. Dewi, and W. A. Adi. 2016. Synthesis, Characterization, and Photocatalytic Activity of Fe₃O₄-ZnO Nanocomposite. *International Journal of Technology* (7 (3): 408–16.
- Winatapura, Dewi S. H, and Ridwan. 2014. Synthesis and Characterization of Fe₃O₄-ZnO Composite through Precipitation Method. *Journal of Waste Management Technology* 17 (1): 71–77.
- Xu, M.g, and C. Li. 2014. Monodisperse Nanostructured of Fe₃O₄/ZnO Microrods Using for Waste Water Treatment. *Advanced Powder Technology* 25: 1–9.
- Xue, C., Q. Zhang, J. Li, X. Chou, W. Zhang, H. Ye, Z. Cui, and P. J Dobson. 2013. High Photocatalytic Activity of Fe₃O₄-SiO₂-TiO₂ Functional Particles with Core-Shell Structure. *Journal of Nanomaterials* 2013: 1–9.